Numerical simulation of particle-fluid flows: Validation and Comparison of Direct model and Drag law model

Vincent Komiwes[1], Christophe Denis[1] and Hans Herrmann[2]

[1] Laboratoire d'Informatique de Paris 6, Université Pierre et Marie Curie - Paris 6, 4 place jussieu, 75252 Paris Cedex 05, France Email: vkomiwes@netscape.net

[2] IfB, ETH Zurich, Schafmattstr.6, 8093 Zurich, Switzerland

Abstract

In order to reliably simulate particle-fluid mixtures on the particle scale, this paper presents the validation and a comparison of two computational methods based on solving the Navier-Stokes coupling with a discrete model for particles.
The fluid models are based on a Navier-Stokes solver around each particle (Direct model) and on a volume-averaged Navier-Stokes solver with a Drag law (Drag law model). After a short review of the models, we validate and compare them by the two following cases: Periodic Stokes flow through porous and Sedimentation with analytical expressions and empirical laws. The purpose is to show the advantages and limitations of the two models. We show that the Drag law model is very efficient in CPU time and requires less memory consumption than the Direct model, but is restricted to the dense media.

Keyword : Computational methods, Numerical simulation, Computational fluid dynamics, Fluid-particle mixture, Projection method, Navier-Stokes, Discrete model, Drag force, Porous media, Sedimentation

1. Introduction

Many problems in industry and science involve granular media interacting in a fluid. In particular, we can quote the industrial separation of an insoluble solid from a liquid or gas, using fluidized beds or sedimentation. The analysis of these problems involves fluid mechanics, the Physics of granular media, Chemistry, applied mathematics and computational science.
Various computational methods have been developed to simulate particle-fluid mixtures depending on the resolution scale. At larger scale than the particle diameter, two fluid continuous models [1], [2], [3] are popular in the engineering sciences.
In these models, questions remain concerning the proper constitutive equation for the solid and the modelling of the momentum transfer between the solid and fluid phases. In general, the momentum transfer is modelled by a local drag force depending on the local relative velocity between the solid and the fluid, the Reynolds number and the local volume fraction of solid and fluid.
This drag law is based on Ergun's law [4] giving the pressure drop in granular media for fixed and fluidized beds.
In the following, we present some computational methods on the particle scale.
The finite element and volume finite methods are very accurate but need remeshing with a very high computional effort [5], [6]. With today's powerful computers it is not yet possible to simulate more than a few hundred particles.
In order to avoid remeshing, uniform grids can be used giving an efficient computational method [7] ,[8], [9], [10], [11], [12], [13], [14], [15].

Recent computational approaches simulating the flow of fluid-solid mixtures, inspired by molecular dynamics, use a Lattice Boltzmann approach. These models have been applied to the simulation of a large number of particles in a fluid by various authors [16], [17].

After a short review of the numerical models, this paper presents the validation and a comparison of two numerical models based on solving the Navier-Stokes coupling with a discrete model for particles. We use a staggered grid for the fluid flow with a computational scale equal to the particle diameter (Drag Law Model) and smaller than the particle diameter (Direct Model). The purpose is to show the advantages and limitations of the two models.

2. Numerical models

We use a discrete model for the particle flow, inspired by molecular dynamics [18]. It computes the particle trajectories through non-dimensional Newton's law as follows:

$$\overrightarrow{f_g} + \overrightarrow{f_{h_0}} + \overrightarrow{f_h} + \overrightarrow{f_n} + \overrightarrow{f_t} = m_{i_p} \frac{d^2 x_{i_p}}{dt^2} \ , \ \ i_p = 1, \ldots, n_p \quad (1)$$

where n_p is the number of particles, m_{i_p} the mass of the particle i_p, f_g the gravity force, f_n and f_t are the collision forces in the normal and tangential direction.
The fluid and the particle are coupled by the hydrodynamic force f_h as discussed in the next sections 2.1 and 2.2. The complete expressions of the other forces and algorithms are given in [15].

2.1. Direct Model

We use the non-dimensional Navier-Stokes equations with a resolution scale h smaller than the particle size to solve the fluid flow around each particles:

$$\frac{\partial v_i}{\partial t} = -\frac{\partial (v_i v_j)}{\partial x_j} - \frac{\partial p}{\partial x_i} + \frac{1}{Re}\frac{\partial^2 v_i}{\partial x_i^2}, \quad \frac{\partial v_i}{\partial x_i} = 0 \quad (2) \ \text{with : } v_i = (v_p)_i \ \text{at the particle surface.}$$

where Re is the Reynolds number defined by: $Re = \rho_f \ V_s \ r/\mu_f$ and $\vec{v}_p$ is the particle velocity.

An explicit operator splitting, fractional-time-step method, first order in time and second order in space discretization are used in to solve the Navier-Stokes equation [19].

The time-step Δt_f for the fluid is given by the stability condition [19]:

$$\Delta t_f = min\left(\frac{h^2 \ Re}{6}, \frac{2}{max(\|\vec{v}\|^2) \ Re} \right) \quad (3)$$

The particle-fluid coupling (momentum transfer between the fluid and the particle) is directly calculated by integrating the stress tensor over the particle surface S and obtained from the hydrodynamic force f_h given by:

$$(f_h)_i = I_S + \vec{f}_{h_0} = \int_S \sigma_{ij} \cdot n_j dS + \frac{4}{3}\pi r^3 Fr \ \vec{u}_{x_2} \quad (4) \quad \text{with } \sigma_{ij} = -p\delta_{ij} + \frac{1}{Re}\left(\frac{\partial v_i}{\partial x_j} + \frac{\partial v_j}{\partial x_i} \right) \quad (5)$$

The integral I_S is computed by decomposing the surface into the quadrangles Q_{h_q} :

$$I_S = \sum_{q=1,q_{max}} \int_{\Omega_{h_q}} \sigma_{ij} \cdot n_j dS \quad (6)$$

To improve the accuracy of our previous work [15], we use a second order trapezoidal formula to compute the integral value. We determine the accuracy of the method in the section 3.1.

2.2. Drag Law Model

This model is derived from the two fluid continuous models commonly used in Engineering science. The fluid flow is computed from the non-dimensional volume-averaged Navier-Stokes equations as follow:

$$\frac{\partial \varepsilon u_i}{\partial t} = -\frac{\partial \varepsilon u_j u_i}{\partial x_j} - \varepsilon \frac{\partial p}{\partial x_i} + \frac{\partial \varepsilon T_{ij}}{\partial x_j} + f_i + \varepsilon g_i \;, \quad \frac{\partial \varepsilon}{\partial t} + \frac{\partial \varepsilon u_i}{\partial x_i} = 0 \quad (7)$$

with : $T_{ij} = \frac{1}{Re}\left(\frac{\partial u_i}{\partial x_j} + \frac{\partial u_j}{\partial x_i}\right) - \frac{2}{3\,Re}\frac{\partial u_q}{\partial x_q}\delta_{ij}$ (8) and $\vec{g} = g_i \vec{u}_{x_2} = -Fr\,\vec{u}_{x_2}$ (9)

where ε is the local average volume fraction of fluid, u_i is the average velocity of the fluid and p is the average pressure of the fluid. As these fields have only physical meaning as averages over volume on a scale of the particles radius, we take $h=2r$ as computational scale.

As for the Direct model, we use the same computational method based on the projection method.

The particle-fluid coupling is described by a drag force f_d and a pressure force term as follows:

$$(f_h)_i = (f_d)_i - \frac{\partial p}{\partial x_i} V_p \quad (10)$$

where V_p is the volume of the particle and the drag force f_d is given by:

$$\vec{f}_d = \frac{1}{2}\pi \rho_f \beta r^2 \left\| \vec{u} - \vec{v}_p \right\| \cdot (\vec{u} - \vec{v}_p) \quad (11) \quad \text{with:} \quad \beta = \begin{cases} C_d \varepsilon^{-2.7} (1 + 0.15\, Re^{0.7}), \varepsilon > 0.8 \\ C_d \left(\frac{25}{3} (1 - \varepsilon) + \frac{1.75}{18} Re \right), \varepsilon \le 0.8 \end{cases} \quad (12)$$

f_i is the source term for the momentum exchange contribution and is obtained by using the actio=reactio principle:

$$f_i = -\sum_{i_p=1,n_c} (f_{d_{i_p}})_i \,\delta(x - x_{i_p}) \quad (13)$$

where x_{i_p} is the position of the particle i_p and n_c is the total number of particles in the cell.

In order to evaluate the fluid velocity field at the location of the particle, we interpolate linearly the fluid velocity using the 8 closest grid nodes:

$$\vec{u}_i(x_{ip}) = \sum_{q=1,8} w(x^q)\, u_i(x^q) \quad (14)$$

where $x_q = (x_1, x_2, x_3)$ is a grid node position and $w(x^q)$ is the weight associated with the particle position $x_{i_p} = (x_{1_{ip}}, x_{2_{ip}}, x_{3_{ip}})$ given by:

$$w(x^q) = \left(1 - \frac{\left|x_{1_{ip}} - x_1^q\right|}{h}\right)\left(1 - \frac{\left|x_{2_{ip}} - x_2^q\right|}{h}\right)\left(1 - \frac{\left|x_{3_{ip}} - x_3^q\right|}{h}\right) \quad (15)$$

By using the same weight, we obtain the following discrete expression for the source term f_i at the grid node x^q:

$$f_i(x^q) = -\frac{1}{h^3}\sum_{ip=1,n_c}\sum_{q=1,8} w(x^q)\left(f_{d_{ip}}\right)_i \quad (16)$$

The same method is used to evaluate the local average volume fraction of the fluid at the location of the particle.

3. Validation and comparison

3.1. Fluid flow through a periodic porous media

In order to estimate the accuracy of the hydrodynamic drag force computation as a function of volume concentration, we consider the case of a Stokes flow through a porous media of fixed spheres. As in our previous work [15], the simulation results are compared with Sangani's analytical expression [20] of the non-dimensional drag K:

$$K^{-1} = 1 - 1.7601\phi^{\frac{1}{3}} + \phi - 1.5593\phi^2 + 3.9799\phi^{\frac{8}{3}} - 3.0734\phi^{\frac{10}{3}} + O\left(\phi^{\frac{11}{3}}\right) \quad (17)$$

and the empirical based Ergun's law [4] with $Re<<1$:

$$K = \begin{cases} (1-\phi)^{-4.7}, & \phi < 0.2 \\ \frac{25}{3}\frac{\phi}{(1-\phi)^3}, & \phi \geq 0.2 \end{cases} \quad (18) \qquad \text{with : } K = \frac{f_h}{6\pi r \mu_f U} \quad (19)$$

where ϕ is the volume concentration of solid, f_h is the modulus of the hydrodynamic force, μ_f is the fluid viscosity and U is the mean fluid velocity. The simulations parameters are the same in [15].

As shown in Figure 1 The improvement of the numerical integration leads to an error in order $O(h^{3/2})$ instead of $O(h)$ in [15] where the error is defined by:

$$Error = \frac{\left|K_{computed} - K_{sangani}\right|}{K_{sangani}} \times 100 \quad (20)$$

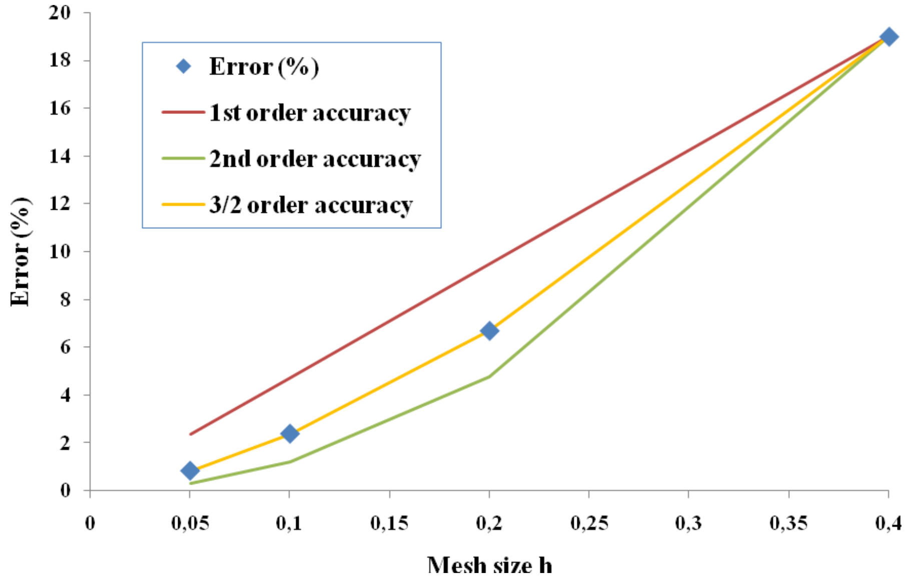

Figure 1. Error as a function of the mesh size h

We see in Figure 2 the simulation of denser media demands a mesh size that decreases with the volume concentration of solid.

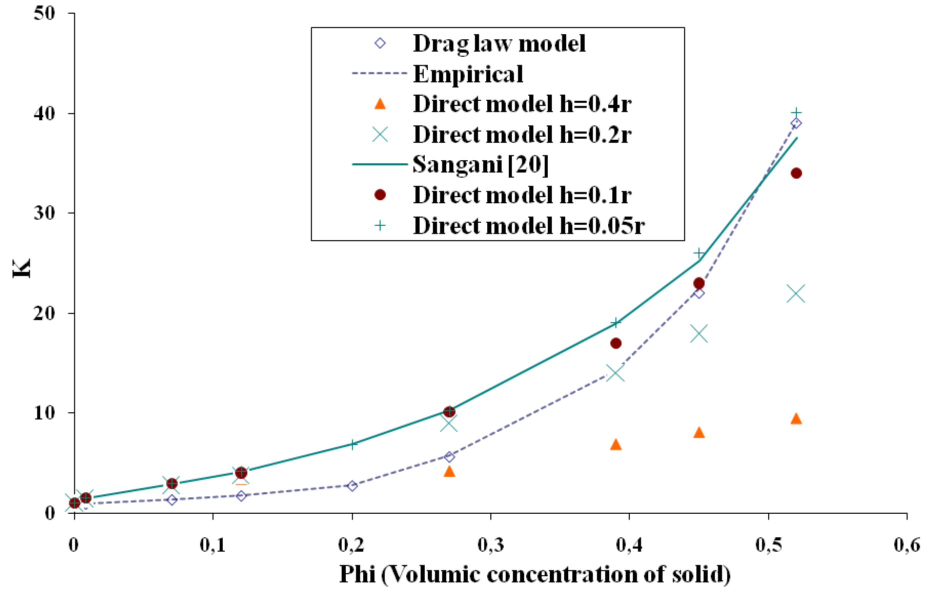

Figure 2. Hydrodynamic drag force K as a function of the volume concentration of solid

The reason for these limitations comes from the fact that the denser the medium, the smaller are the pores through which the fluid can pass requiring a smaller resolution.

For the Drag law model, simulations are in good agreement for the dense medium (ϕ>0.4), but not for the intermediate and diluted medium where simulations more closely match, unsurprisingly, the empirical expression equation (18).

We conclude that the Drag law model is more appropriate for the dense medium and the Direct model for the dilute and intermediate medium.

3.2. Sedimentation

In the following, we compare the Richardson and Zaki [21] law with the simulations of a system of particles sedimenting in a fluid: $v_m(\phi)=V_0(1-\phi)^n$ (21)

where V_0 is the velocity of an isolated particle and v_m is the mean velocity of particles.
The physical parameters is given in the section 3.3.
The simulations done with the Drag law model and the Direct model yield the law for different volume concentrations (see Figure 3).

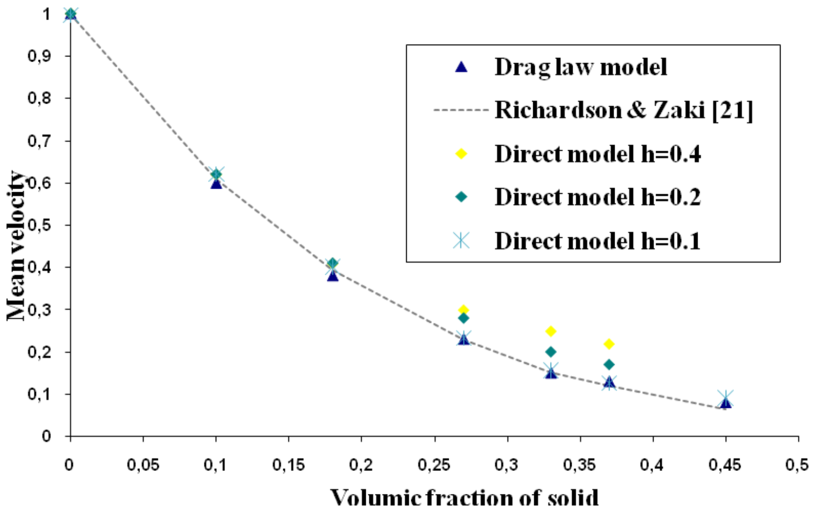

Figure 3. Mean sedimentation velocity as function of volume concentration.

We see the simulation of denser media demands a mesh size that decreases with the volume concentration of solid.
Due to this limitation, we conclude that the Direct model is more appropriate to simulate dilute or intermediate media ($\phi<0.4$).

Figure 4 illustrates respectively the pressure and the velocity field of the flow in the region $x_3 = Lx_3/2$, $0 \leq x1 \leq Lx_1/2$ and $0 \leq x_2 \leq Lx_2/4$.
The depression zone corresponds to negative values of fluid pressure shown by Figure 4.

The differences of particle locations between both simulations result from the underestimation of the hydrodynamic force of the Drag law model.

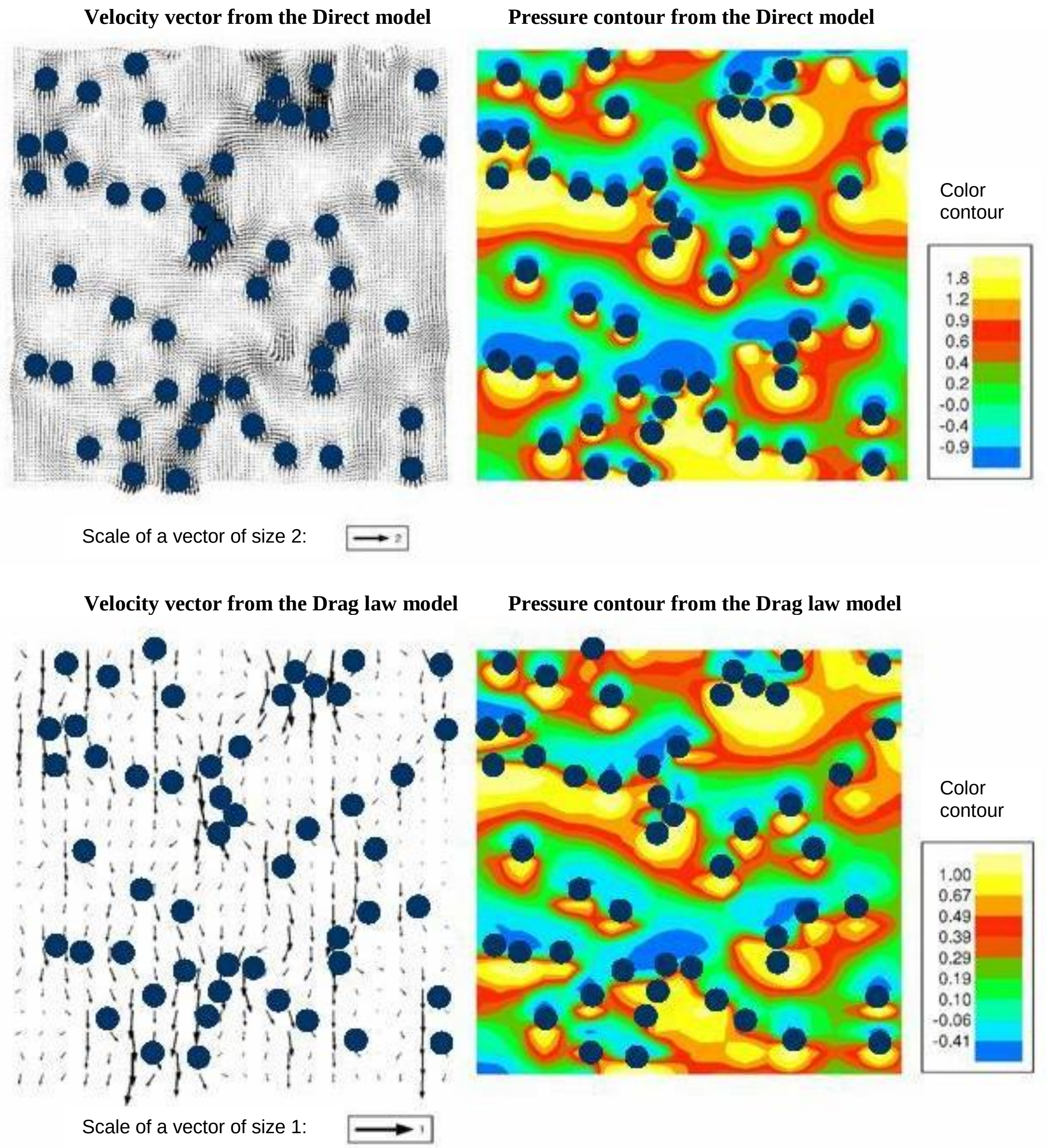

Figure 4. The left and right part illustrate respectively the velocity vector and the pressure field of the fluid at x3 $=Lx_3/2$, $0 \leq x1 \leq Lx_1/2$ and $0 \leq x2 \leq Lx_2/4$ with a mesh size h1 = 0.4r from the Direct model (above) and from the Drag law model (below).

3.3. Benchmarks

A typical case of a gas-solid simulation on a SUN Ultra SPARC workstation is given by the following physical parameters:

$\rho_f = 1.2\ kg \cdot m^{-3}$, $\rho_p = 1500\ kg \cdot m^{-3}$, $\mu_f = 1.8 \times 10^{-5}\ kg \cdot s \cdot m^{-1}$, $d_p = 100\ \mu m$.

The dimensions of the simulation box are: $L_{x1} = 24r$, $L_{x2} = 72r$, $L_{x3} = 24r$.

In this case a number of particles of $n_p=500$, a simulation of a physical time $t=0.1s$ with $h=0.4r$ takes about *82h* of CPU time and *110 Mo* of Memory for the Direct model software and less than *13mn* and less *0.5 Mo* than for the Drag law model. We use a super computer for a smaller mesh size with the Direct model.

4. Conclusions and future-work

The applications allow to validate the Direct model and discern the limitations on the volume concentrations of solid, the mesh size, the memory and CPU time consumption.
Due to the mesh size limitation, the Direct model is more appropriate to simulate dilute and intermediate medium. The simulation of the Direct model allows to find a good agreement with the analytical expressions for the hydrodynamic force of flow through porous media for intermediate volume concentrations of solid. The hydrodynamic drag is computed with an error of order $O(h^{3/2})$.
The simulation of the Drag law model is not accurate enough to find a good agreement with the analytical expressions of the hydrodynamic force of flow through porous media for intermediate volume concentrations of solid.
We show that the Drag law model is very efficient in CPU time and requires less memory consumption than the Direct model, but is restricted to the dense media.

5. Acknowledgments

The authors thank Stephan Schwarzer of the Institut für Computerphysik in Stuttgart for several motivating discussions and for contributions to the initial version of the simulation code. Vincent Komiwes thanks Laurent Giraud of Bouygues Telecom, Gilles Ferschneider and Hakim Koudil of the IFP, Fabienne Jezequel and Laurent-Stephane Didier of LIP6 for enlightening discussions.
Vincent Komiwes thanks Eric Clement of LMDH for his advice.

References

[1] G. Ferschneider, P.Mege. Eulerian, 1996. Simulation of Dense Phase Fluidized Beds. Oil & Gas Science and Technology - Rev. IFP, Vol. 51, No. 2, 301-307.

[2] O. Simonin, 5th Workshop on two phase flow predictions, 19-22-03/90, Erlangen RFA

[3] S. Soo, 1967. Fluid dynamics of multiphase systems, Baisdell Publishing Co

[4] S.Ergun, 1952. Fluid flow through packed columns. Chemical Engineering Progress, Vol. 48, 89-94.

[5] H.H. Hu, D.D. Joseph, A.F. Fortes, 1992. Experiments and direct simulations of fluid particle motions, Int. Video J. Eengineering Research, Vol. 2, 17-24.

[6] R. Glowinski, T.W. Pan, T.I. Hesla, D.D. Joseph, J. Periaux, 2001. A fictitious domain approach to the direct numerical simulation of incompressible viscous flow past moving rigid bodies: Application to particulate flow, *J. Comput. Phys.*, Vol. 169, 363-426.

[7] Hoomans, B.P.B., Kuipers, J.A.M., Briels, W.J. and van Swaaij, 1996. Discrete Particle Simulation of Bubble and Slug Formation in a Two-Dimensional Gas-Fluidised Bed: A Hard Sphere Approach. *Chem. Eng. Sci.*, Vol. 51, No.1, 99-110.

[8] W. Kalthoff, S. Schwarzer, G. Ristow, and H. Herrmann, 1996. On the application of a novel algorithm to hydrodynamic diffusion and velocity fluctuations in sedimenting systems. Int. J. Mod. Phys. C, Vol. 7, No. 4, 543–561

[9] S. Schwarzer, 1995 Sedimentation and flow through porous media: Simulating dynamically coupled discrete and continuum phases, Phys. Rev. E, Vol. 52, 6461 - 6475

[10] Y.Tsuji, T.Tanaka, 1993. Discrete particle simulation of flow patterns in two-dimensinal gas fluidized beds. Int. J. Mod. Phys B, Vol. 7, 1889-1898

[11] Xu, B. H., Yu, A. B., Chew, S. J. and Zulli, P. (2000) Numerical simulation of the gas-solid flow in a bed with lateral gas blasting. Powder Technology, Vol. 109, 13-26

[12] K.Höfler and S.Schwarzer, 2000. Navier-Stokes simulation with constraint forces: Finite-difference method for particle-laden flows and complex geometries, Phys. Rev. E, Vol. 61, 7146 – 7160

[13] B.Wachmann, W.Kalthoff, S.Schwarzer, H.J.Herrmann, 1998. Collective drag and sedimentation: comparison of simulation and experiment in two and three dimensions Granular Matter, Vol.1, No. 2, 75-82

[14] F. Fonseca, H.J. Herrmann, 2005. Simulation of the sedimentation of a falling oblate ellipsoid, Physica A Vol. 345, 341-355

[15] V. Komiwes, P. Mege, Y. Meimon, H.J. Herrmann, 2005. Simulation of granular flow in a fluid applied to sedimentation, Granular Matter Vol. 8, 41-54

[16] A. J. C. Ladd and R. Verberg, 2001. Lattice-Boltzmann simulations of particle-fluid suspensions. J. Stat. Phys., Vol. 104, 1191-1251

[17] Jens Harting, Martin Hecht, Hans J. Herrmann, Sean McNamara, 2006. Computer simulation of particle suspensions Multifield Problems in Solid and Fluid Mechanis, Lecture Notes in Applied and Computational Mechanics , Springer

[18] H.J. Herrmann, 1993. Molecular dynamics simulations of granular materials, Int. J. Mod. Phys. C, Vol. 4, 309-316

[19] R. Peyret and T.D. Taylor, 1993. Computational Methods for Fluid Flow, Springer Series in Computational Physics, Springer

[20] A.S. Sangani and A. Acrivos, 1982. Slow flow through a periodic array of spheres, Int. J. Multiphase Flow, Vol. 8, No. 4, 343-360

[21] J.F. Richardson and W.N. Zaki, 1954. Sedimentation and Fluidization : Part 1. Trans. Instn. Chem. Engrs, Vol. 32, 35–53